

A NEW DIGITAL LLRF SYSTEM FOR A FAST RAMPING STORAGE RING*

Manuel Schedler, Frank Frommberger, Wolfgang Hillert, Dennis Proft,
Dennis Sauerland, ELSA, University of Bonn, Germany
Dmitry Teytelman, Dimtel Inc., San Jose, USA

Abstract

At the Electron Stretcher Facility ELSA of Bonn University, an upgrade of the maximum stored beam current from 20 mA to 200 mA is planned. The storage ring operates applying a fast energy ramp of 6 GeV/s from 1.2 GeV to 3.5 GeV and afterwards a slow beam extraction over a few seconds to the hadron physics experiments. The intended upgrade is mainly limited by the excitation of multibunch instabilities. As a countermeasure, we successfully commissioned state-of-the-art bunch by bunch feedback systems in the longitudinal and the two transverse dimensions.

To achieve the maximum feedback gain, the beam phase with respect to the reference signal and the synchrotron frequency has to stay constant. A high performance low level RF system has been commissioned which is able to stabilize voltage and phase of the RF station while in addition taking care of resonator resonance tuning using a fast FPGA based fully digital approach.

THE ELECTRON STRETCHER ACCELERATOR – ELSA

ELSA is a three-stage electron accelerator. One of the two linear accelerators is used to inject an electron beam of 20 MeV into a fast ramping booster synchrotron to gain an energy of typically 1.2 GeV. The beam can be accumulated and stored in the 164.4 m long stretcher ring, accelerated to a maximum energy of 3.5 GeV and, finally, slowly extracted to the hadron physics experiments using resonance extraction methods [1]. The main operating parameters of the accelerator are summarized in Table 1.

The typical ramping speed of (4–6) GeV/s applied in the stretcher ring generates special requirements for the LLRF system, which will be discussed in this proceeding.

REQUIREMENTS FOR THE NEW LLRF

The stretcher ring's RF station consists of two five-cell normal conducting PETRA type RF cavities, driven by a single klystron with a maximum output power of 250 kW. The power is coupled into a waveguide system and split via a magic T into two equal parts for both cavities.

The injection rate of 200 mA/s delivered by one of the linear accelerators in combination with a fast ramping 50 Hz booster synchrotron at 1.2 GeV leads to rapid changes in beam loading of the RF cavities. In addition, the fast energy ramp of up to 6 GeV/s produces significant variation in synchrotron frequency and beam synchronous phase. A typical

Table 1: Main Operating Parameters of the ELSA Stretcher Ring

parameter	value
Length	164.4 m
RF	499.669 MHz
Bunch spacing	2 ns
Harmonic number h	274
Filled buckets	274
Revolution frequency f_{rev}	1.8236 MHz
Beam energy E	(1.2 – 3.5) GeV
Beam current	(20 – 200) mA
Ramping speed	≤ 6 GeV/s
Injection rate	50 Hz
Momentum compaction factor α_c	0.063

ELSA booster mode operation cycle including fast injection and ramping is shown in Figure 1.

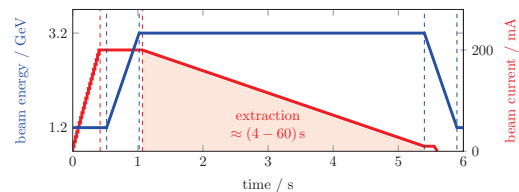


Figure 1: Typical ELSA booster mode operation cycle for extraction to hadron physics experiments.

The high intensity upgrade of the stretcher ring is mainly limited by coupled bunch instabilities, especially in the longitudinal plane. In order to damp those instabilities at high beam currents a state-of-the-art bunch by bunch feedback system has been installed in 2009. This system analyzes the motion of every single bunch every turn in the stretcher ring and calculates a correction signal to damp existing oscillations. A fast kicker applies the correction signal to the beam. Feedback performance is significantly degraded by the above-mentioned shifts in the synchrotron frequency and synchronous phase.

Synchrotron radiation loss per turn U_{rev} scales as E^4 , where E is the beam energy. During the fast energy ramp the beam's phase φ_s changes with respect to the accelerating RF voltage U according to

$$U_{\text{rev}} = U \cdot \sin(\varphi_s). \quad (1)$$

* Work supported by the DFG within the SFB/TR 16

At the same time, synchrotron frequency during ramping changes as follows [2]:

$$f_s = f_{rev} \sqrt{\frac{e\alpha_c h}{2\pi} \frac{U \cos \varphi_s}{E}} \quad (2)$$

To compensate for the changes in f_s it is sufficient to scale $U \propto E / \cos \varphi_s$. To maintain constant beam phase relative to the master oscillator, RF accelerating field must be shifted in phase as $\sin^{-1}(U_{rev}/U)$. Thus, the LLRF system must be able to adjust both amplitude and phase of the accelerating voltage during energy ramping according to analytically calculated profiles. Proper synchronization of the energy and RF ramps requires a hardware trigger in the LLRF system.

OVERVIEW OF THE NEW LLRF SYSTEM

The new LLRF9/500 system, developed and manufactured by Dimtel, Inc. [3] and based on the LLRF4.6 evaluation board was commissioned at ELSA in October 2013. Nine highly stable wideband RF inputs are used to monitor RF cavity and waveguide signals. Two cavity probe signals are used in a digital feedback loop to stabilize the vector sum of the accelerating cavity voltages. The input channel allocation and function is summarized in Table 2.

Table 2: Overview of the Digitized RF Input Signals

channel	signal	purpose
1	cavity 1 probe 1	RF and tuner loop
2	cavity 2 probe 1	RF and tuner loop
3	cavity 1 probe 2	balancing loop
4	cavity 2 probe 2	balancing loop
5	cavity 1 forward	tuner loop
6	cavity 1 reflected	monitoring
7	cavity 2 forward	tuner loop
8	cavity 2 reflected	monitoring
9	klystron forward	monitoring

The LLRF system is based on a fully digital approach. All of the nine analog RF inputs are digitized after down conversion to $\frac{1}{12}$ of the RF ≈ 42 MHz and processed by the FPGA. The cavity field stabilization is performed by two feedback loops: the low-latency proportional and the integral. The detailed layout of the FPGA feedback processing is described in [4].

Fully digital approach provides 10 Hz monitoring of amplitude and phase for each input signal. The FPGA continuously compares all input signals with the adjustable interlock thresholds. With the intermediate frequency of 42 MHz the maximum latency for detecting an interlock event is limited to 96 ns. Every interlock event is latched and time stamped. Fast data acquisition with pre-trigger capture provides information for postmortem analysis. The FPGA generates a trip signal which, together with an external interlock input, controls an RF switch disabling the klystron drive output.

An internal state machine handles the system operation. On interlock trip, system setpoint is automatically set to zero and the feedback loops are opened. An orderly station startup is then possible after trip event is analyzed and cleared.

The new LLRF unit is internally temperature controlled in order to prevent amplitude and phase drifts. All of the critical RF components are mounted on a 10 mm thick cold plate with active Peltier temperature stabilization.

HARDWARE TRIGGERED VOLTAGE AND PHASE RAMPING

FPGA uses 512 point amplitude and phase setpoint tables to support transient RF field ramping. A table address counter selects the current station setpoint. The setpoint state machine supports four modes of operation: first table entry, last table entry, ramping up or down. The first two modes continue operating until a hardware or software trigger is received, initiating a “first to last” or “last to first” transition. Transition times from 9 μ s to 18.7 s are produced using an adjustable delay per step. Two opto-isolated trigger inputs allow the integration of the LLRF system into the global ELSA cycle timing. For example, during nominal energy ramp from 1.2 GeV to 3.2 GeV, the RF voltage is ramped up within 330 ms from 971 kV to 2.71 MV. To keep the beam’s phase fixed with respect to the RF master oscillator, the RF phase of the accelerating fields is ramped as well by -17.2° .

TUNER LOOPS

Mechanical tuner control is critical for compensating beam loading changes during injection and energy ramping. The new LLRF system implements PID control of two tuner motors per cavity, operating at 10 Hz. The tuner loop acts to keep the cavity probe and forward signals in phase for minimum reflected power. ELSA mechanical tuners are actuated by stepper motors, controlled via RS-485 bus.

Common-mode motion of the two tuners within one five-cell cavity controls the resonant frequency of the fundamental mode. Differential motion can be used to adjust the field distribution in individual cells. A balancing loop adjusts differential tuner positions to maintain an appropriate ratio between probe signals in the center and side cells.

Fast injection and fast ramping pose an especially challenging problem for the mechanical tuning system. At the present time the tuning loops have latencies on the order of 100–200 ms. The planned beam current increase will require faster tuner control which is currently being investigated.

DIAGNOSTICS CAPABILITIES

Time Domain

Each input channel can be captured in a 16 k sample buffer with flexible pre- and post-trigger acquisition. This functionality is used for a variety of system setup and diagnostic functions. Here we illustrate two such applications: post-trigger acquisition for feedback step response measurement and pre/post-trigger capture during interlock events.

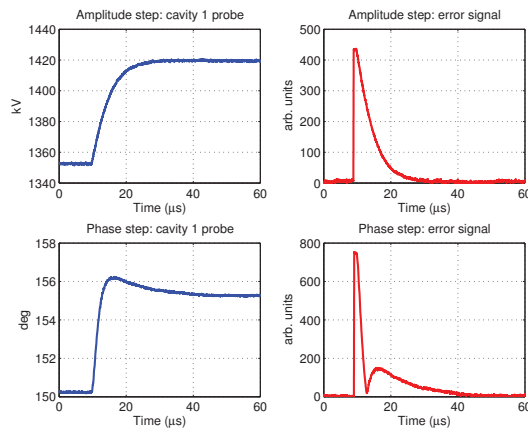


Figure 2: Closed-loop step response measurement.

Figure 2 shows the response to a 5% amplitude step from 1.35 MV to 1.42 MV per cavity and to a phase step from 150° to 155° . Amplitude step response is somewhat underdamped with 15 μs settling, whereas the phase step response overshoots. This discrepancy is explained by klystron saturation, which results in reduced amplitude modulation gain, while phase modulation is unaffected.

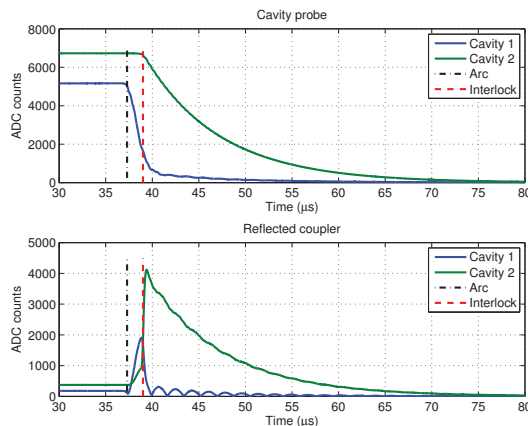


Figure 3: Example of a captured interlock event at ELSA, with an arc in cavity 1 triggering reflection interlock.

Figure 3 shows an interlock event captured during ELSA operation at an accelerating voltage of 1.65 MV per cavity. At about 37 μs into the record, a gas discharge generates reflected power in cavity 1, resulting in an interlock trip at 39 μs . Note the rapid decay in cavity 1 probe signal as compared to cavity 2, which shows the expected exponential decay corresponding to the loaded quality factor of $\approx 14\,000$. After RF drive is removed, cavity 2 generates large reflected power, as expected. Meanwhile the stored energy in cavity 1 has been mostly dissipated in the arc, with only a small fraction reflected to the waveguide.

Frequency Domain

A digital swept-sine network and spectrum analyzer is integrated in the LLRF system. This unit complements the

time-domain diagnostics described above. In the network analyzer mode, a sinusoidal excitation is added to the station setpoint and the system's response is detected at the same frequency. Selectable measurement inputs include cavity probes, feedback loop error signal, and klystron drive. Resulting magnitude and phase transfer functions are used for system setup, e.g. tuner and feedback loop configuration, as well as for performance characterization.

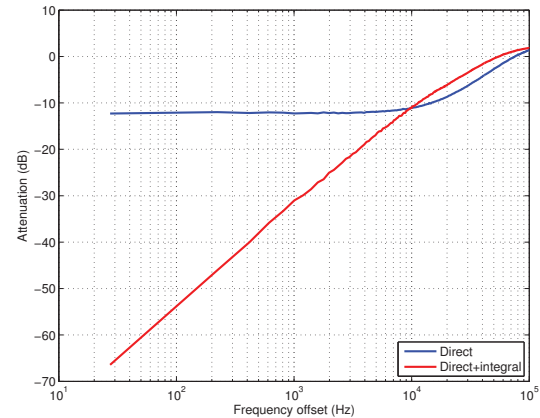


Figure 4: Internal network analyzer measurement showing error suppression with and without integrator.

Figure 4 shows two magnitude transfer functions measured from the station setpoint to the loop error signal. These responses characterize feedback rejection of perturbations as a function of frequency. Horizontal axis shows the offset from the RF frequency. Direct loop achieves 13 dB rejection below 10 kHz. Turning on the integral loop provides additional rejection at low frequencies, achieving 65 dB at 30 kHz offset. Since integral loop has higher latency than the direct loop, it slightly reduces feedback rejection above 10 kHz.

CONCLUSION

The new LLRF system matches exactly the requirements for the ELSA booster cycle operation. Both the fast tuner loop and the field stabilization support fast injection of the desired beam current and the fast energy ramp, required in order to gain a duty cycle of $\approx 80\%$ of the extracted beam current. Using bunch-by-bunch feedback in three planes in combination with the new LLRF system, we achieved stable operation at a beam current of 242 mA at injection energy. This marks a promising step in the path to high intensities.

REFERENCES

- [1] W. Hillert, The Bonn Electron Stretcher Accelerator ELSA: Past and future, *Eur.Phys.J. A28S1*, 139 (2006)
- [2] B.J. Holzer, Introduction to Longitudinal Beam Dynamics arXiv:1404.0927 [physics] (2014)
- [3] Dimtel, Inc., San Jose, USA, <http://www.dimtel.com>
- [4] D. Sauerland, et al., Amplitude, Phase and Temperature Stabilization of the ELSA RF System, *IPAC'13 Conf. Proc.* (2013) 2717